

A NEW DIGITAL FEEDBACK AND FEEDFORWARD CONTROLLER FOR CAVITY FIELD CONTROL OF THE LANSCE ACCELERATOR

Sungil Kwon[#], L. Castellano, D. Knapp, M. Prokop, P. Torrez, A. Scheinker, and J. Lyles
 Los Alamos National Laboratory, Los Alamos, New Mexico, USA

Abstract

Many conference series have adopted the same A new digital low-level RF system (LLRF) was designed and deployed on the drift-tube-linac section of the Los Alamos Neutron Science Center (LANSCE) proton accelerator. This new system is part of a modernization of the existing analog cavity-field controls that were originally developed and put into service forty-five years ago. For stabilization of the cavity field amplitude and phase during beam loading, a proportional-integral feedback controller, a static beam feedforward controller, and an iterative learning controller working in parallel have been implemented. In this paper, the controller architecture is described, and the performances of the three controllers when beam is being actively accelerated is presented.

INTRODUCTION

The modernization of the LANSCE 201 MHz RF systems including the LLRF control systems, RF amplifier systems was performed[1]. Analog low level RF control and electronics have been replaced with FPGA based control systems. The new design of the LLRF system consists of an FPGA with an embedded softcore processor and network support. In addition, the FPGA-based design gives the ability for algorithm and processor modification and upgrade. For the regulation of the cavity field, PI feedback controller is implemented as a default controller. In order to improve the performance for beam loading, a static feedforward controller and a iterative learning controller are implemented. Figure 1 shows the overall control system block diagram. In this note, the features of the controllers are addressed and the performance of controllers for the LANSCE production beam operation is presented.

CAVITY MODEL

When beam is not loaded, the transfer function of the open loop system is expressed as

$$G(s) = \begin{bmatrix} \frac{g_{I0}}{\tau s + 1} e^{-T_d s} & 0 \\ 0 & \frac{g_{Q0}}{\tau s + 1} e^{-T_d s} \end{bmatrix} \quad (1)$$

where T_d is the loop delay, g_{I0} and g_{Q0} are I channel and Q channel steady state gains[2,3]. The time constant, τ , can be estimated based on the open loop system step response[2]. The LLRF system generates a pulse and it is exerted after the cavity field reaches its steady state. The pulse perturbs the cavity field and the cavity field perturbation is used to obtain the time constant of the cavity.

[#] skwon@lanl.gov

Figure 2 shows the test data scope shot. Cavity field (magenta) is in steady state at 400usec. At that instant, a pulse(yellow) is exerted, resulting in the cavity field perturbation. The cavity field waveform is uploaded to the host computer via EPICS channel access (CA). From cavity field amplitude waveform data, the time constant and the 3db bandwidth of the cavity are obtained: $\tau = 79.51\text{usec}$, $f_{3dB} = 2002\text{Hz}$.

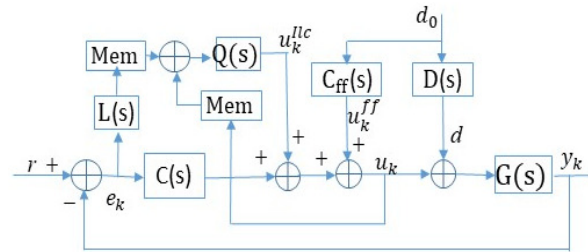


Figure 1: Overall Control Block Diagram.

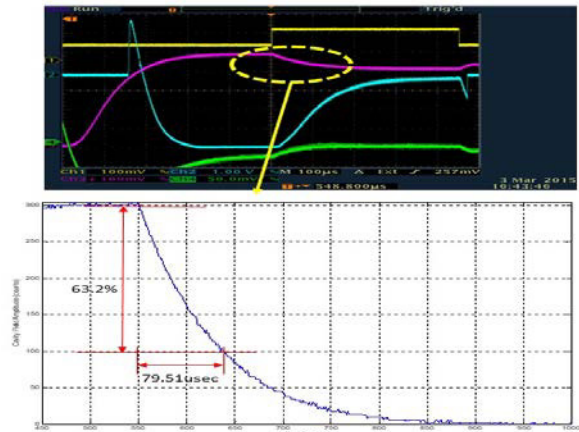


Figure 2: Cavity Bandwidth Estimation.

FEEDBACK CONTROL

The transfer function $C_D(z)$ of the implemented discrete time PI controller is expressed as

$$C_D(z) = \frac{K_P}{2^{13}} + \frac{K_I}{2^{15}} \frac{1}{1-z^{-1}} \quad (2)$$

Here, the proportional gain K_P and integral gain K_I are 16 bit unsigned integers. The corresponding transfer function $C(s)$ of the continuous time PI controller can be obtained by $s = \frac{z-1}{t_s}$ where t_s is the sampling time. The performance of the PI control system is shown Figure 3. Note that with higher PI gains, better performance is obtained. However, since there is a loop delay of 3usec, gains are chosen not to degrades robustness stability. Figure 4 shows the relation between the PI controller gains and the loop delay. For fixed proportional gains of I and Q channels, as the integral gains are increased, the peak magnitude of the

Content from this work may be used under the terms of the CC BY 3.0 licence (© 2018). Any distribution of this work must maintain attribution to the author(s), title of the work, publisher, and DOI.

Content from this work may be used under the terms of the CC BY 3.0 licence (© 2018). Any distribution of this work must maintain attribution to the author(s), title of the work, publisher, and DOI.

sensitivity function, $S(s) = (1 + G(s)C(s))^{-1}$ of the closed loop system[4], is pushed toward the higher frequency region and the excitation amount of the modes of the loop delay is increased, resulting in oscillation of the time response of the closed loop system.

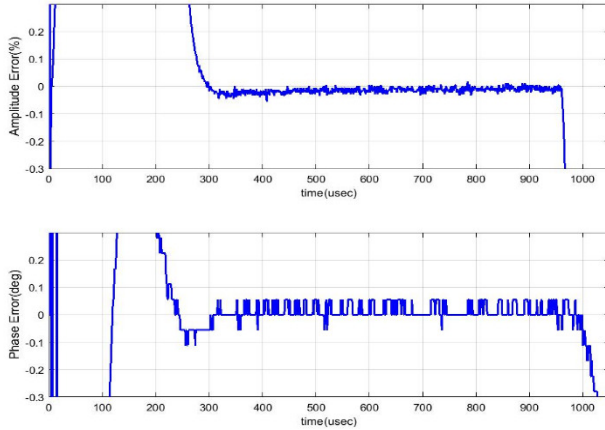


Figure 3: PI feedback controller performance.

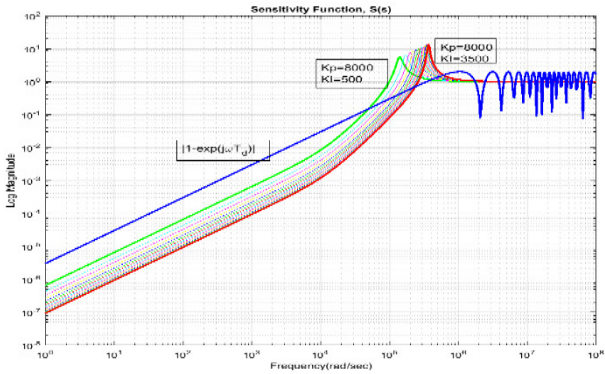


Figure 4: Sensitivity Function dependency on integral Gain. The loop delay is 3usec.

BEAM FEEDFORWARD CONTROL

Two types of beam loading compensation feedforward controllers are implemented. The first feedforward controller is the static beam feedforward controller, where the detected beam current is read-back to the LLRF system and a proper amplification and rotation of the detected beam current generates the feedforward I and Q control signals. Since the plant of our application is two-input two-output (TITO) system, two static feedforward controllers are necessary for both I channel and Q channel.

$$C_{ff}(s) = \begin{bmatrix} K_{ff}^I \frac{B_{ff}^I s + 1}{T_{ff}^I s + 1} & 0 \\ 0 & K_{ff}^Q \frac{B_{ff}^Q s + 1}{T_{ff}^Q s + 1} \end{bmatrix} e^{-L_{ff}s} \quad (3)$$

Ideal static beam feedforward controller parameters are

$K_{ff}^I = g_d^I / g_{I0}$, $K_{ff}^Q = g_d^Q / g_{Q0}$, $B_{ff} = \tau$, $T_{ff} = \tau_{dist}$ and $L_{ff} = T_{dist} - T_d$. Here, g_d^I , g_d^Q , τ_{dist} and T_{dist} are I channel and Q channel steady state gains, the time constant and loop delay of the disturbance dynamics, respectively.

It is known that when $T_{dist} > T_d$, the perfect control is

achieved[5]. When $T_{dist} < T_d$ which is our case, the feedforward controller is time-advanced and other special approach such as generalized predictive control(GPC) which needs heavy computational capability[5,6] or a classical approach that takes away the time delay part in Eq. (3).

ITERATIVE LERNING CONTROL

The iterative learning controller(ILC) of the form Eq. (4) is implemented[7,8].

$$u_{k+1}^{ILC} = \alpha Q(u_k + Le_k) \quad (4)$$

where u_k is the input to the plant and it is the sum of the iterative learning controller output, feedforward controller output, and the feedback controller output.

$$u_k = u_k^{ILC} + Ce_k + u_k^{FF} \quad (5)$$

In Figure 1, the output of the system is given by

$$y_k = G(u_k + d) \quad (6)$$

By applying Laplace transform to Eq.(6), we obtain the frequency response of the closed loop system for the repetitive disturbance, $D = D_k = D_{k+1}$,

$$\begin{aligned} Y_k &= G(U_k + D) \\ &= G(U_k^{ILC} + CE_k + U_k^{FF} + D) \\ &= T_R R + T_U U_k^{ILC} + T_D D \end{aligned} \quad (7)$$

where

$$T_R = \frac{GC}{1+GC}, \quad T_U = \frac{G}{1+GC}, \quad T_D = \frac{G}{1+GC} \quad (8)$$

By applying Laplace transform to Eq. (4) and Eq. (5), we obtain the frequency response of the system input

$$\begin{aligned} U_{k+1} &= U_{k+1}^{ILC} + CE_{k+1} + U_{k+1}^{FF} \\ &= \alpha Q(U_k + LE_k) + CE_{k+1} + U_{k+1}^{FF} \\ &= \frac{\alpha Q(1-LG)}{1+GC} U_k + \frac{\alpha QL+C}{1+GC} R + \frac{1}{1+GC} (U_{k+1}^{FF} - (\alpha QL + C)GD) \end{aligned} \quad (9)$$

If the disturbance is bounded, that is, if $\|d_k\| \leq \beta$, $k = 0, 1, 2, \dots$, for a constant β , the sufficient convergence condition of the input Eq. (9) is

$$\alpha \left\| \frac{Q(1-LG)}{1+GC} \right\|_{\infty} < 1 \quad (10)$$

and when u_k converges, then the iterative learning control u_k^{ILC} also converges. Figure 5 shows the dependence of the convergence Eq. (10) upon the parameter α where Q filter is first order low pass IIR filter and $L = 1$. In the LLRF system, the ILC is implemented with fixed point data format and the integer data format parameter α as shown in Figure 5 is divided by 1024 resulting in the floating point α . Note that the condition Eq. (10) is satisfied for all α or Q , if L -filter is designed as $L = G^{-1}$. The asymptotic error converges when the control converges.

$$\begin{aligned} \lim_{k \rightarrow \infty} E_k &= \frac{1-\alpha Q}{1+GC-\alpha Q(1-LG)} R \\ &+ \frac{G}{1+GC-\alpha Q(1-LG)} ((\alpha Q - 1)D - U_{k+1}^{FF}) \end{aligned} \quad (11)$$

Ideally, the plant parameters are exactly known and the L -filter is designed as $L = G^{-1}$. Then, Eq. (11) is reduced to

$$\lim_{k \rightarrow \infty} E_k = \frac{1-\alpha Q}{1+GC} R + \frac{G}{1+GC} ((\alpha Q - 1)D - U_{k+1}^{FF}) \quad (12)$$

Equations (11) and (12) show that unless $\alpha = 1$ and Q is an all-pass filter, the reference effect to the asymptotic error remains. Further, when the static feedforward control is adjusted in such a way that the right hand side of Eq. (11)

or Eq. (12) makes zero, the error converges to zero. Currently, the LANSCE accelerator accelerates 4 beam species [9]. Each beam has different features in length, chopping, magnitude, rate, etc.. The ILC, shown in Figure 6, updates the future control output based on the current control output and the current error. The error and the control output are stored in a memory for the future control output computation. Different beam produces different error and therefore for each beam, its own error/control output memories are allocated. Those memory reading and writing are enabled by the beam species. The Q filter of the iterative learning controller is applied commonly to all beam.

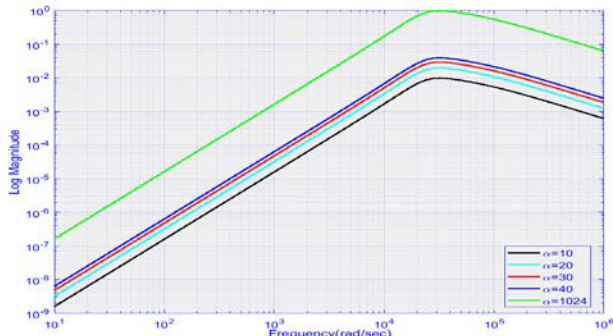


Figure 5: Control Convergence Condition of Iterative Learning Control. Q filter is a low pass filter and $L=1$.

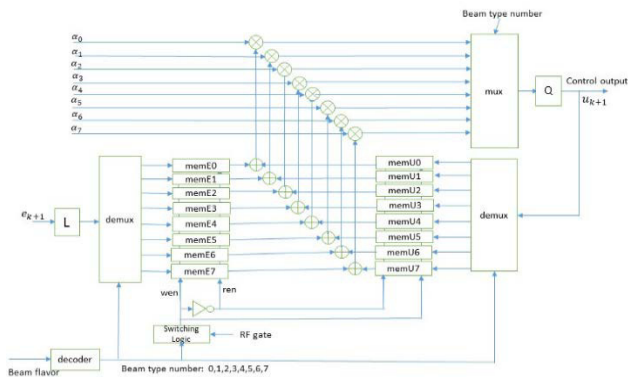


Figure 6: Iterative Learning Controller structure implemented on the LLRF FPGA.

BEAM PRODUCTION EXPERIMENTS

For the beam loading test, α is adjusted manually via calculating the error norm in such a way that the error norm is decreasing. Figure 7 shows the ILC performance for the Isotope Production Facility (IPF) beam consisting of 3.8 mA (peak) H+ beam. A discrete time first order low pass IIR filter is implemented for Q-filter, whose pole is 0.305. Note that $\alpha = 0$ is when only PI controller and static beam feedforward controller are applied. The error data is obtained inside the LLRF FPGA. Figure 8 shows the performance of the ILC for 8.0mA H- 1LTarget (LBEG) beam after the ILC converges. The amplitude error and phase error are obtained with ADL5511 [10] and the AD8302 [10], respectively. Figure 9 shows the dependency of the ILC performance upon the Q-filter pole (3db bandwidth) with LBEG beam. The figure shows that as the pole of the discrete time Q-filter becomes more close to 1.0, the peak

amplitude error increases. This means that as the Q-filter becomes narrower, the higher frequency error spectrum is filtered and the ILC cannot suppress this error spectrum.

CONCLUSION

The digital LLRF system has been installed at LANSCE 201MHz DTL tanks. The compensation performances of iterative learning control yields more than 100% improvement of the amplitude and phase stability over the feedback plus static feed forward performance for the LANSCE H+ and H- beam loading.

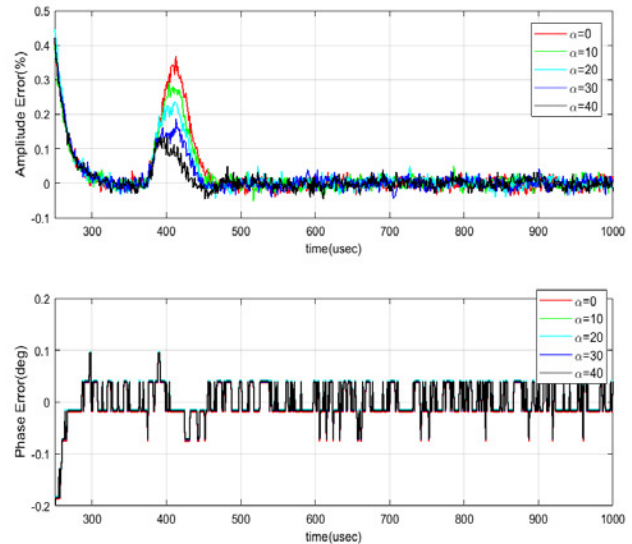


Figure 7: ILC Performance for 3.8mA H+ beam.

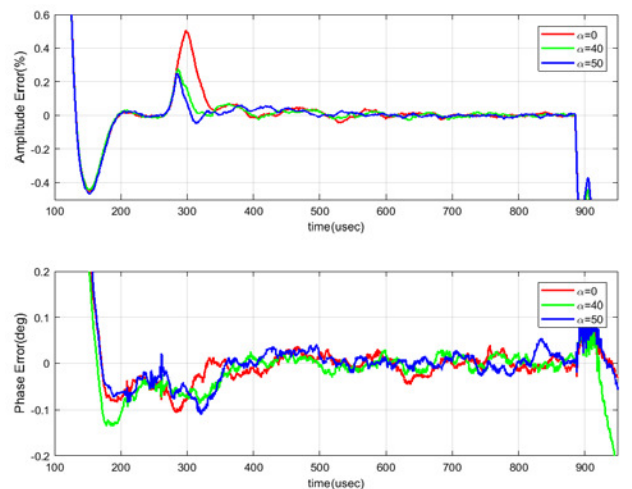


Figure 8: ILC Performance for 8mA H- beam.

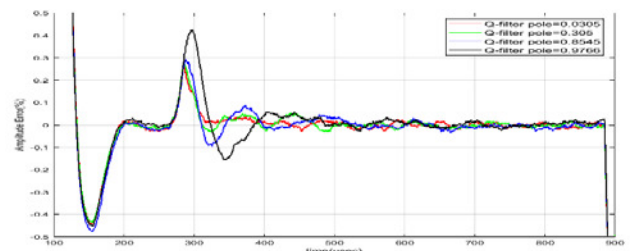


Figure 9: The dependency of ILC Performance on the Q filter bandwidth. $\alpha = 40$.

REFERENCES

- [1] J. Lyles *et al.*, “Installation and Operation of Replacement 201 MHz High Power RF System at LANSCE,” IPAC 2015, Richmond, VA, USA.
- [2] Kwon, Sung-il, Lynch, Mike, and Prokop, Mark, “Decoupling PI controller for a normal conducting RF cavity using a recursive LEVENBERG-MARQUARDT algorithm,” IEEE Trans. Nuclear Science, vol. 52, no. 1, 2005.
- [3] Feng Qiu, *et al.*, “Application of disturbance observer-based control of low-level radio-frequency system in a compact energy recovery linac at KEK,” Physical Review Special Topics-Accelerator and Beams, vol.18, no.9, 2015.
- [4] Sigurd Skogestad and Ian Postlethwaite, Multivariable Feedback Control: Analysis and Design, John Wiley & Sons, Ltd., 1996.
- [5] J.L. Guzman and T. Hagglund, “Simple tuning rules for feed forward compensators,” Journal of Process Control, vol.21, pp. 92-102, 2011.
- [6] Andrzej Pawlowski, *et al.*, “Measurable Disturbances Compensation: Analysis and Tuning of Feedforward Techniques for Dead-Time Process,” Process, vol.4, no.12 pp1-20, 2016.
- [7] Sungil Kwon, Amy Regan, and Yi-Ming Wang, “SNS Superconducting RF cavity modeling-iterative learning control,” Nuclear Instruments and Methods in Physics Research Section A, vol. 482, pp12-31, 2002.
- [8] M. Verwoerd *et al.* “On admissible pairs and equivalent feedback-Youla parameterization in iterative learning control,” Automatica, vol.42, pp2079-2089, 2006.
- [9] Mark Prokop, Sungil Kwon, Phillip Torrez, and Stephen Ruggles, “LANSCE-R low level RF control system, PAC2007, Albuquerque, NM, USA.
- [10] Analog Devices, <http://www.analog.com>